

## **I. EXECUTIVE SUMMARY**

## **2. INTRODUCTION**

### 3. DATA SOURCES

Report cards are typically compiled and communicated annually. However, the time window that constitutes a year differs from report card to report card. Many environmental report cards communicate on data collected within a financial year. This schedule provides a reporting window that is consistent with other management and governmental considerations. Others use a time window that naturally aligns with the cycle of some major underlying environmental gradient - such as wet/dry season. For this project, we are adopting using the same water year (1st Oct – 31 Sept) definition as the AIMS inshore Water Quality Marine Monitoring Program (Lønborg et al., 2016).

The Great Barrier Reef Marine Park (GBR) spans nearly 14° of latitude and covers approximately 344,400km<sup>2</sup>.

- spanning multiple jurisdictions/pressures as well as distance offshore - more useful to partition the GBR into smaller more homogeneous zones representing combinations of region and water body. - Six regions (Cape York, Wet Tropics, Dry Tropics, Mackay Whitsunday, Fitzroy and Burnett Mary) - Four water bodies (Enclosed Coastal, Open Coastal, Midshelf and Offshore) - define each...

Table 1: Great Barrier Reef spatial Zones and associated Regions and Water bodies.

GBRMPA Zone	Zone	Region	Water body
Enclosed_Coastal_Cape_York	Enclosed_Coastal_Cape York	Cape York	Enclosed Coastal
Enclosed_Coastal_Terrain_NRM	Enclosed_Coastal_Wet Tropics	Wet Tropics	Enclosed Coastal
Enclosed_Coastal_Burdekin_Dry_Tropics_NRM	Enclosed_Coastal_Dry Tropics	Dry Tropics	Enclosed Coastal
Enclosed_Coastal_Mackay_Whitsunday_NRM_Group	Enclosed_Coastal_Mackay Whitsunday	Mackay Whitsunday	Enclosed Coastal
Enclosed_Coastal_Fitzroy_Basin_Association	Enclosed_Coastal_Fitzroy	Fitzroy	Enclosed Coastal
Enclosed_Coastal_Burnett_Mary_Regional_Group_for_NRM	Enclosed_Coastal_Burnett Mary	Burnett Mary	Enclosed Coastal
Open_Coastal_Cape_York	Open_Coastal_Cape York	Cape York	Open Coastal
Open_Coastal_Terrain_NRM	Open_Coastal_Wet Tropics	Wet Tropics	Open Coastal
Open_Coastal_Burdekin_Dry_Tropics_NRM	Open_Coastal_Dry Tropics	Dry Tropics	Open Coastal
Open_Coastal_Mackay_Whitsunday_NRM_Group	Open_Coastal_Mackay Whitsunday	Mackay Whitsunday	Open Coastal
Open_Coastal_Fitzroy_Basin_Association	Open_Coastal_Fitzroy	Fitzroy	Open Coastal
Open_Coastal_Burnett_Mary_Regional_Group_for_NRM	Open_Coastal_Burnett Mary	Burnett Mary	Open Coastal
Midshelf_Cape_York	Midshelf_Cape York	Cape York	Midshelf
Midshelf_Terrain_NRM	Midshelf_Wet Tropics	Wet Tropics	Midshelf
Midshelf_Burdekin_Dry_Tropics_NRM	Midshelf_Dry Tropics	Dry Tropics	Midshelf
Midshelf_Mackay_Whitsunday_NRM_Group	Midshelf_Mackay Whitsunday	Mackay Whitsunday	Midshelf
Midshelf_Fitzroy_Basin_Association	Midshelf_Fitzroy	Fitzroy	Midshelf
Midshelf_Burnett_Mary_Regional_Group_for_NRM	Midshelf_Burnett Mary	Burnett Mary	Midshelf
Offshore_Cape_York	Offshore_Cape York	Cape York	Offshore
Offshore_Terrain_NRM	Offshore_Wet Tropics	Wet Tropics	Offshore
Offshore_Burdekin_Dry_Tropics_NRM	Offshore_Dry Tropics	Dry Tropics	Offshore
Offshore_Mackay_Whitsunday_NRM_Group	Offshore_Mackay Whitsunday	Mackay Whitsunday	Offshore
Offshore_Fitzroy_Basin_Association	Offshore_Fitzroy	Fitzroy	Offshore
Offshore_Burnett_Mary_Regional_Group_for_NRM	Offshore_Burnett Mary	Burnett Mary	Offshore

Table 2: Summary of used data sources.

Source	Custodian	Description
AIMS Insitu	AIMS	AIMS inshore monitoring program Niskin data
AIMS FLNTU	AIMS	AIMS inshore monitoring program FLNTU logger data
Satellite	BOM	BOM: Catalog <a href="http://ereefds.bom.gov.au/ereefs/tds/catalog/ereef/mwq/PID/2002/catalog.html">http://ereefds.bom.gov.au/ereefs/tds/catalog/ereef/mwq/PID/2002/catalog.html</a>
eReefs	eReefs	<a href="#">provide a description in ../parameters/sources.csv</a>
eReefs926	eReefs	eReefs: <a href="http://dapds00.nci.org.au/thredds/catalog/fix3/gbr4_bgc_926/catalog.html">http://dapds00.nci.org.au/thredds/catalog/fix3/gbr4_bgc_926/catalog.html</a>

#### 3.1 Indicators

One of the biggest challenges of report card development is the selection of appropriate indicators from amongst a potentially very large candidate pool. Since the outcomes, conclusions and implications are all dependent on the indicators selected, the selection process is one of the most influential steps and has justifiably received a great deal of attention.

As part of their ecosystem report card framework, Harwell et al. (1999) urged that the alignment of scientific information with societal goals and objectives should be the guiding principal of indicator selection. In their framework, clearly articulated societal goals and objectives (a combination of societal values and scientific knowledge, such as restored and sustainable wetland system) are translated into Essential Ecosystem Characteristics (EECs)

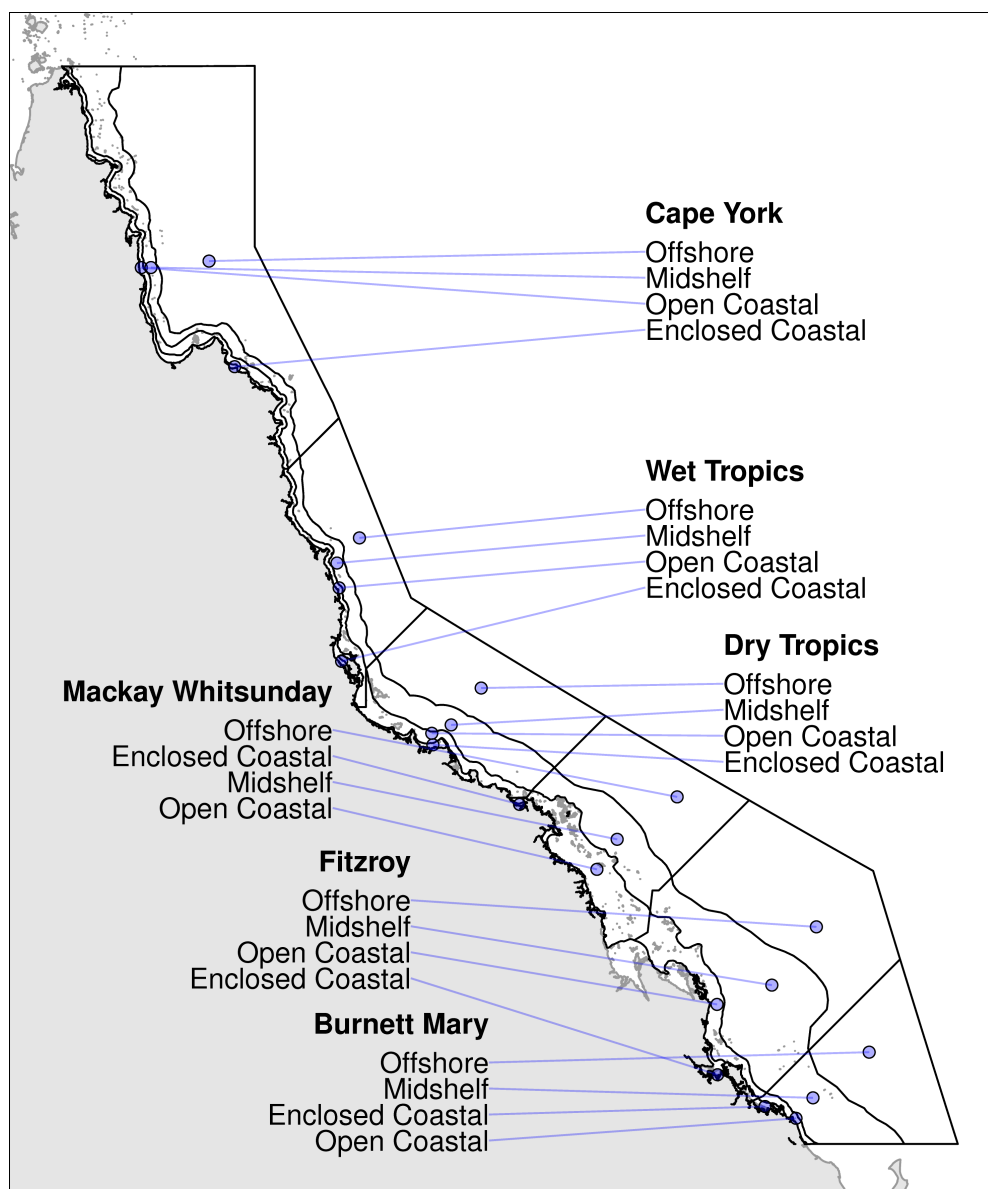


Figure 1: Great Barrier Reef Zones (Regions and Water Bodies).

that represent a set of generic attributes that further refine the broad goals (such as water quality, sediment quality, habitat quality, ecological processes). The EEC's are then further translated into a set of scientific informed indicators that are measured or monitored to indicate the status of trends or states associated with the EEC's.

There have since been numerous studies that have focused on providing more formal, objective criterion for indicator selection (Dauvin et al., 2008; Emerson et al., 2012; Flint et al., 2012; James et al., 2012). Whilst the specifics vary, most can be broadly encapsulated by a Dauvin et al. (2008)'s contextual implementation of the Doran (1981)'s SMART (Simple, Measurable, Achievable, Realistic, and Time limited) principle. A 'good' indicator should be representative, easily interpreted, broadly comparable, sensitive to change and have a reference or guideline value. To be 'useful', an indicator must be approved by international consensus, be well grounded and documented, have a reasonable cost/benefit ratio and have adequate historical and on-going spatial-temporal coverage. Flint et al. (2012) and James et al. (2012) further developed numerical scoring systems to help evaluate indicators objectively. Nevertheless, (Neary, 2012) warned against the potential to manipulate an index by saturating with inappropriate or biased indicators and whilst recommending that an index comprise of at least seven indicators, they did advocate that the type of indicator is more important than the number of indicators.

Since final outcomes are likely to be highly influenced by indicator choice, the robustness and sensitivity of both indicators and final outcomes to changes in ecosystem health should be understood if not formally investigated as part of the indicator selection process (Dobbie and Dail, 2013). Sensitivity analyses can involve:

- simulating changes in the underlying data of different magnitudes and estimating the resulting sensitivity (percentage or probability of change) expressed by the indicator
- estimating the effect of past perturbations on the indicator hindcasted from on historical data

As stressed above, indicators should align intimately with report card objectives. Yet in the more broad ecosystem report card frameworks, such indicators are often too general to be measurable. Therefore, in such cases, the indicators are further sub-divided into progressively more specific measures. For example, an indicator of water quality might comprise sub-indicators of nutrients, metals and physico-chemistry which in turn might be represented by more specific measures such as total nitrogen, mercury, dissolved oxygen, pH etc.

The resulting design is a hierarchical structure in which sub-indicators (etc) are nested within indicators and spatial scales are nested from entire regions, sub-regions or zones down to individual sites or sampling units. One of the strengths of such a hierarchical report card framework is that the inherent inbuilt redundancy allows for the addition, deletion or exchange of finer scale items (sites and actual measured variables) with minimum disruption to the actual report indicators. That is, the indicator is relatively robust to some degree of internal makeup. Furthermore, by abstracting away the fine details of an indicator, similar indicators from different report cards (each potentially comprising different sampling designs) are more directly comparably. For example, in different report cards that include water quality, a water quality indicator of 'water clarity' might comprise different Measures (e.g. suspended solids, NTU, Secchi depth etc) collected from different sources (e.g. satellite, in situ loggers or hand samples), yet provided each of these water clarity indicators are well calibrated, it should be possible to compare state and trend across the report cards.

Table 3: Water Quality Measure hierarchy specifying which Measures contribute to which Subindicators and which Subindicators contribute to which Indicators.

Indicator	Subindicator	Measure	Label	Units
Water Quality	Productivity	chl	Chlorophyll	$\mu\text{gL}^{-1}$
Water Quality	Water Clarity	nap	TSS	$\text{mgL}^{-1}$
Water Quality	Water Clarity	ntu	NTU	NTU
Water Quality	Water Clarity	sd	Secchi	m
Water Quality	Nutrients	NOx	NOx	$\mu\text{gL}^{-1}$

### 3.2 AIMS insitu samples

The AIMS component of MMP inshore water quality monitoring sampling program has been designed to quantify spatial and temporal patterns in inshore water quality, particularly in the context of catchment loads. Details of the sampling design are outlined in (Lønborg et al., 2016). From 2006–2014, AIMS visited 20 sites, three times per year (roughly corresponding to wet, early and late dry seasons), see Figures 2 and 3. The sites were largely

selected along approximate north-south transects proximal to major rivers so as to provide samples along an expected water quality gradients (exposure to runoff). Following a review in 2014, the design was modified to intensify the spatial (32 sites) and temporal (typically between 5 and 10 samples per year) coverage of the sampling program. In particular, additional sampling effort was applied around three priority focal areas (Russell-Mulgrave, Tully and Burdekin).

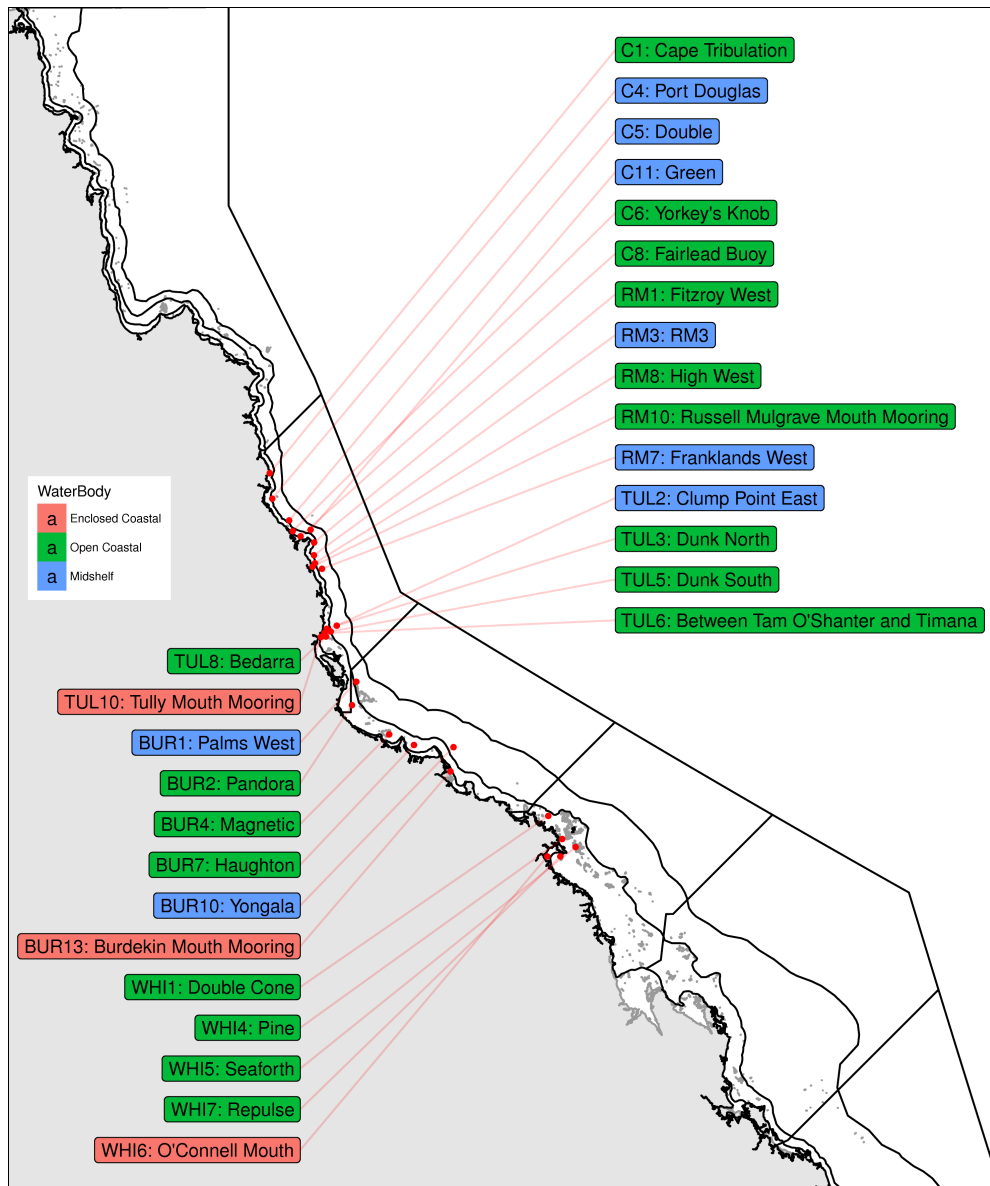


Figure 2: Map of AIMS in situ samples.

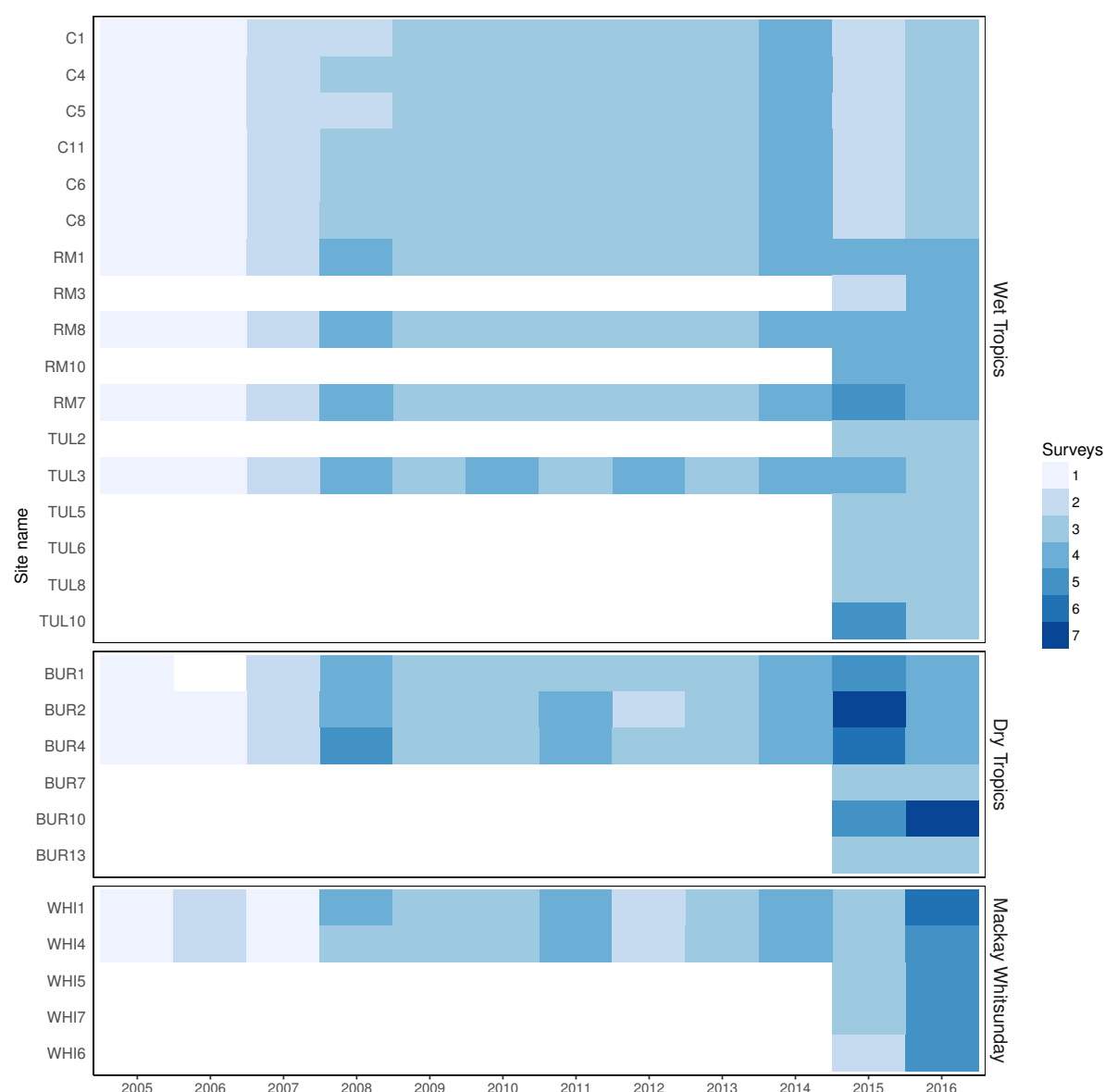


Figure 3: Spatial and temporal distribution of AIMS in situ samples. Sites names follow Great Barrier Reef Marine Park Authority (GBRMPA) and sites are arranged north to south into the focal Regions. Blue shading of tiles denotes the number of surveys conducted in the year at each site.

Table 4: Measures collected in AIMS MMP in situ inshore water quality monitoring program. NO<sub>x</sub> is the sum of NO<sub>2</sub> and NO<sub>3</sub>. Data used are annual means of depth weighted averages per site.

Measure	Variable	Description	Abbreviation	Conversion	Units
Chlorophyll-a	DRIFTCHL_UGPERL.wm	Chlorophyll-a (µg/L)	chl	x1	µgL <sup>-1</sup>
Total Suspended Solids	TSS_MGPERL.wm	Suspended solids (mg/L)	nap	x1	mgL <sup>-1</sup>
Secchi Depth	SECCHI_DEPTH.wm	Secchi depth (m)	sd	x1	m
NO <sub>x</sub>	NOX.wm	Nitrite and Nitrate measured by microanalyser (µM/L)	NO <sub>x</sub>	x14	µgL <sup>-1</sup>

### 3.3 AIMS FLNTU samples

Combination continuous Fluorometer and Turbidity Sensors (hereafter FLNTU) loggers were deployed at 15 of the AIMS MMP inshore water quality monitoring sites.

Table 5: Measures collected in AIMS MMP flntu inshore water quality monitoring program. Data used are daily means per site.

Measure	Variable	Description	Abbreviation	Conversion	Units
Chlorophyll-a	CHL_QA_AVG	??	chl	CHL_QA_AVG x I	$\mu\text{gL}^{-1}$
NTU	NTU_QA_AVG	??	ntu	NTU_QA_AVG x I	NTU

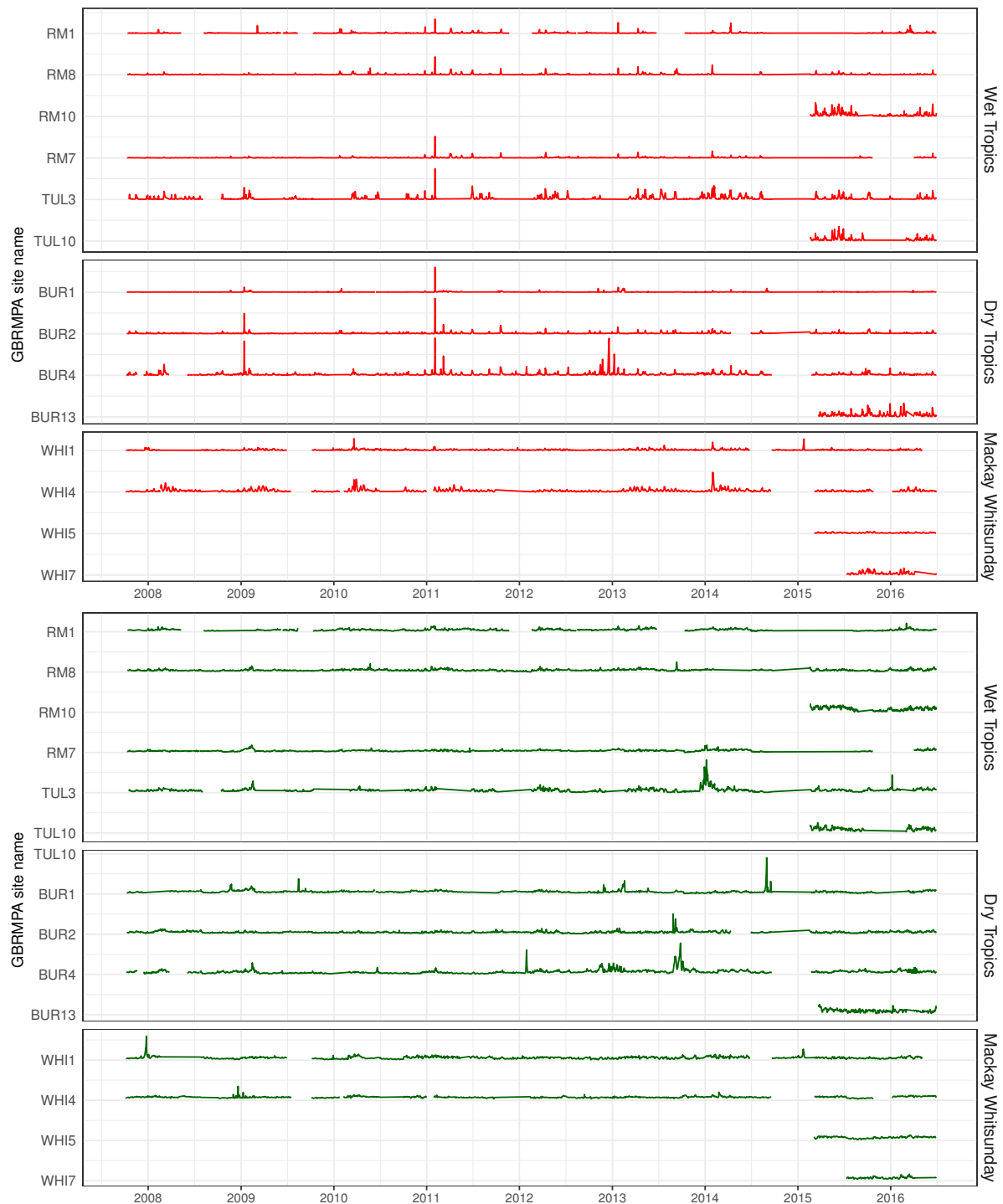


Figure 4: Spatial and temporal distribution of AIMS FLNTU samples (Red: NTU, Green: Chlorophyll-a). Sites names follow Great Barrier Reef Marine Park Authority (GBRMPA) and sites are arranged north to south into the focal Regions.



### 3.4 Remote sensing (BOM satellite)

Daily (July 2002–Dec 2016,  $1 \times 1 \text{ km}^2$  resolution) Moderate Resolution Imaging Spectroradiometer (MODIS satellite) imagery (hereafter referred to as Satellite) data were obtained by downloading NETCDF files from the thredds server.

Table 6: Measures collected from MODIS satellite imaging. Data used are daily means per pixel. Variable and Description pertain to the eReefs source. Conversion indicates the conversion applied on data to conform to threshold Units. Abbreviation provides a consistent key across data.

Measure	Variable	Description	Abbreviation	Conversion	Units
Chlorophyll-a	Chl_MIM	??	chl	Chl_MIM x 1	$\mu\text{g L}^{-1}$
Non-Algal Particles	Nap_MIM	??	nap	Nap_MIM x 1	$\text{mg L}^{-1}$
Secchi Depth	SD_MIM	??	sd	SD_MIM x 1	m

### 3.5 eReefs coupled hydrodynamic -- biogeochemical model

- We need a table that specifies and explains the naming of the various eReefs models and where they are available

The eReefs coupled hydrodynamic, sediment and BGC modelling system involves the application of a range of physical, chemical and biological process descriptions to quantify the rate of change of physical and biological variables (Fig. 5, Schiller et al. (2014)). The processes descriptions are generally based either on a fundamental understanding of the process (such as the effect of gravity on circulation) or measurements when the process is isolated (such as the maximum division rate of phytoplankton cells at  $25^\circ\text{C}$  in a laboratory mono-culture). The model also requires as inputs external forcings, such as observed river flows and pollutant loads. Thus, the model can be run without observations from the marine environment and in this mode is quite skilful (Skerratt et al. (submitted 9 Nov. 2017) and below). This mode which does not use observations from the marine environment as the simulation is undertaken is referred to as the non-assimilating simulation. Most of the eReefs marine biogeochemical simulations are non-assimilating.

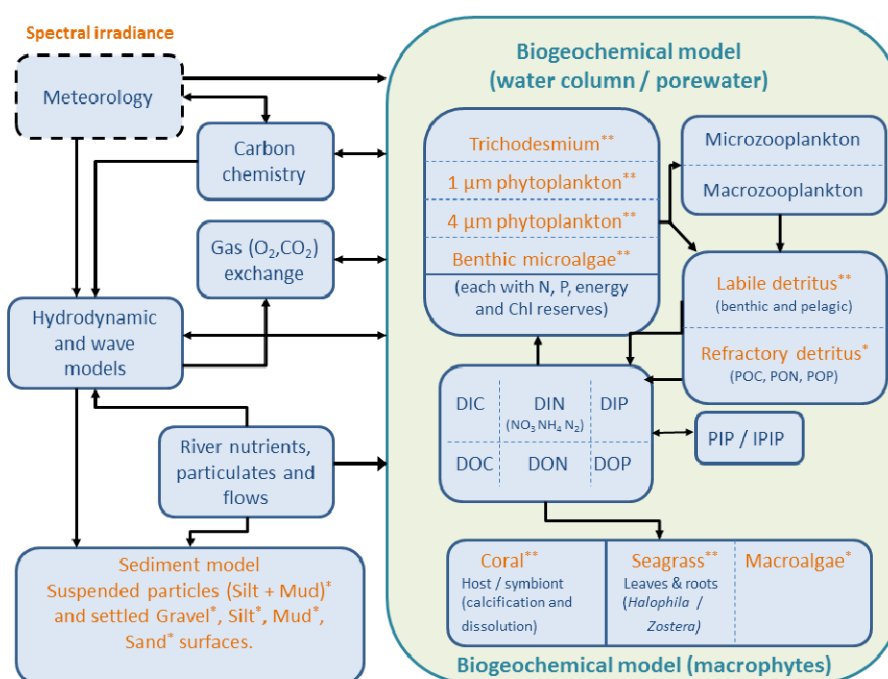


Figure 5: Schematic showing eReefs coupled hydrodynamic biogeochemical model.

Despite being already skilful, the predictive skill of the model can be improved by assimilating marine observations into an ensemble (i.e. a large number (108) of similar but not identical) of model simulations. The form of data

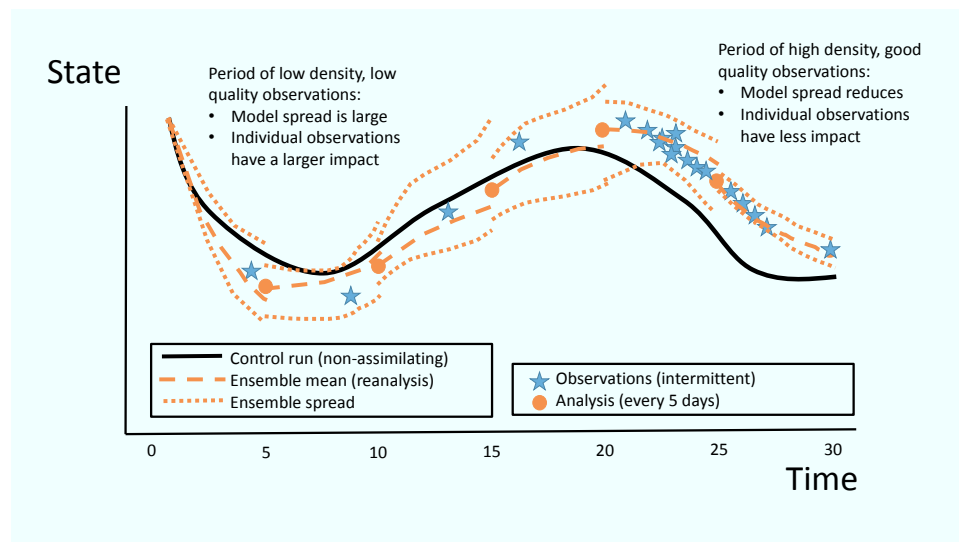


Figure 6: Schematic showing the evolution of the model ensemble over 6 assimilation cycles using the Ensemble Kalman Filter (EnKF) system. The non-assimilating control run (black line) is capturing the gross cycle in the observations (blue stars), but errors remain that observations can constrain. At the initial time, all ensemble members, and the control run, have similar values. In the first five days the 108 members develop a spread, with the control run being different to the ensemble mean, but within the ensemble spread. At 5 days, the first state updating occurs. In the first 5 days there was only one observations, being above the ensemble mean. At day 5, a new state for the entire ensemble is calculated (the analysis being the mean of the updated ensemble) based on the mismatch between the ensemble members and observations. The updated state is closer to the model if the ensemble spread is small, or to the observations if they are dense with few errors. At day 5, because of the small positive mismatch, the ensemble spread is only slightly narrowed, and the mean increased. The ensemble members all restart from these new updated states. The next four analysis steps proceed much like the first. For the fifth analysis step, high density observation were available over the previous 5 days, so the analysis is weighted heavily toward the observations, and the model spread is constrained significantly. Looking at the error between the ensemble mean and the observations over the entire period we see that the data assimilation system has provided an improved estimate of the state (the mean of the ensemble) relative to the control run, and achieved this using the model that contains the processes we understanding to describe system.

assimilation we chose, and that is commonly used in weather forecasting, involves updating of the state of the model as the simulation progresses (Fig. 6). State updating involves first looking for a mismatch between the state of the ensemble members and the observations over the previous 5 days. Ocean colour, the observation of water-leaving irradiance at 8 individual wavebands, provides the only data set with sufficient temporal (daily) and spatial (1 km) resolution, providing upwards of 13 million pixels on a cloud-free day. For this comparison, we have chosen to use the mismatch between the model's prediction of the ratio of the water-leaving irradiance at 443 nm (blue) and 551 nm (green) and the observation of the same quantities from the MODIS sensor on NASA's Aqua satellite. The eReefs biogeochemical model is the first published model to assimilate raw ocean colour observations (Jones et al., 2016). The data assimilation algorithm uses the model-observation mismatch, as well as statistically-quantified dynamical properties of model, to periodically alter the values in the 108 member ensemble, resulting the ensemble mean gaining a closer match to the observations. The outcome of this modelling system is referred to in the field of data assimilation as a reanalysis.

Below we describe the model itself, and then particular data assimilation system.

### 3.5.1 eReefs coupled model description and forcing

The hydrodynamic model is a fully 3-D finite-difference baroclinic model based on the 3-D equations of momentum, continuity and conservation of heat and salt, employing the hydrostatic and Boussinesq assumptions (Herzfeld, 2006; Herzfeld et al., 2015). The sediment transport model adds a multilayer sediment bed to the hydrodynamic model grid and simulates sinking, deposition and resuspension of multiple size classes of suspended sediment (Margvelashvili, 2009; Margvelashvili et al., 2016). The complex BGC model simulates optical, nutrient, plankton, benthic organisms (seagrass, macroalgae and coral), detritus, chemical and sediment dynamics across

the whole GBR region, spanning estuarine systems to oligotrophic offshore reefs (Fig. 5, Baird et al. (2016)). An expanded description of the BGC model is given in Appendix A, with a brief description of the optical model in Appendix B. Briefly, the BGC model considers four groups of microalgae (small and large phytoplankton, Trichodesmium and microphytobenthos), two zooplankton groups, three macrophytes types (seagrass types corresponding to *Zostera* and *Halophila*, macroalgae) and coral communities.

Photosynthetic growth is determined by concentrations of dissolved nutrients (nitrogen and phosphorous) and photosynthetically active radiation. Microalgae contain two pigments (chlorophyll a and an accessory pigment) and have variable carbon : pigment ratios determined using a photoadaptation model (described in Baird et al. (2013)). Overall, the model contains 23 optically active constituents (Baird et al. (2016); and Appendix A).

The model is forced with freshwater inputs at 21 rivers along the GBR and the Fly River in southwest Papua New Guinea. River flows are obtained from the DERM (Department of Environment and Resource Management) gauging network. Nutrient concentrations flowing in from the ocean boundaries were obtained from the CSIRO Atlas of Regional Seas (CARS) 2009 climatology (Ridgway et al., 2002).

The nutrient loads (TSS, PN, PP, DIN, DIP) for the 21 rivers were obtained from the process-based Source models used for Paddock 2 Reef (P2R) load reduction estimates (Waters et al., 2014). The P2R represent land uses and landscape processes in a variety of ways, often based upon spatially explicit farm-scale models that are included through a system of bespoke pre-processing and transfer tools. These P2R Source models also include flow related in-stream processing of pollutants, thus altering loads as fluxes transfer throughout the network. P2R modelling includes scenarios designed to represent 'baseline' (or 'current condition') and 'pre-development' catchment loads. In this report we only use 'baseline' condition. The reliance of the base P2R Source models on external, farm scale sub-models, means that they cannot be easily modified to extend the period covered by the report card. Thus we only use the P2R outputs from Jan 2011 - July 2014.

In order to provide daily timeseries predictions of pollutant loads past July 2014, the reliance on external sub-models was replaced by pollutant generation models that estimate daily loads through monthly varying concentrations ('EMC/DWC'). The particular concentration values for each pollutant for each Functional Unit (FU) within each subcatchment have been calculated by analysing the monthly runoff volumes and pollutant loads from the P2R Source models defined in Waters et al. (2014). The network transport and in-stream processing mechanisms are unaltered from the base P2R Source models. These monthly concentration pollutant generation models allow the model predictions to be extended by providing updated rainfall runoff model inputs (i.e. the runoff of the day), without the need to also update many thousands of farm scale sub-models. Simple comparisons of predicted loads indicates that the monthly varying concentration approach works reasonably well for sediment and associated particulate nutrient, and less well for pollutants that are usually reliant on farm scale representation of management inputs.

### 3.5.2 Assimilation system

#### 3.5.2.1 Assimilation of ocean colour

Ocean colour was chosen as the data set to assimilate due to its availability over the entire GBR at high temporal and spatial density. Ocean colour has often been used for biogeochemical data assimilation (Kidston et al., 2013). In global biogeochemical data assimilation applications, the observation - model mismatch used has often been satellite estimates of *in situ* chlorophyll concentration versus model predicted chlorophyll concentration (Ford et al., 2012). This approach is problematic in coastal waters such as the GBR, where chlorophyll concentration is often overestimated by satellite algorithms due to bottom reflectance or absorption by non-phytoplankton components (Schroeder et al., 2012). So it is not possible in this application to base the data assimilation system on the mismatch of model chlorophyll against satellite estimates of *in situ* chlorophyll. Instead, we have pioneered the use of remote-sensing reflectance as the variable to determine the mismatch between the observed and modelled quantities (Jones et al., 2016).

Remote-sensing reflectance,  $R_{rs}$ , is the ratio of the water-leaving irradiance in the direction of a satellite to the water entering radiance. In this sense it is a 'raw' satellite observation. The value of  $R_{rs}$  varies with wavelength and is measured in  $\text{sr}^{-1}$  ( $\text{sr}$  = steradians, the SI unit of solid angle, where the solid angle in all direction on a spherical surface is  $4\pi \text{ sr}$ ). In the open ocean at blue wavelengths the value is around  $0.03 \text{ sr}^{-1}$  (Baird et al., 2016). That is, 3 % of the light that entered the ocean within  $1 \text{ m}^2$  emerged travelling in the direction within a solid angle of  $1 \text{ sr}$  (i.e.  $1/4\pi$  of a sphere).

The model contains 23 optically active constituents (shaded orange in Fig. 5, see also Baird et al. (2016)). For each of these constituents the optical model calculates the rate of absorption, scattering and backscattering. To

calculate  $R_{rs}$  at the surface, we need to consider the light returning from multiple depths, and from the bottom. Rather than using a computationally expensive radiative transfer model, we approximate  $R_{rs}$  based on an optical-depth weighted scheme (Baird et al., 2016). The model sums the return from each depth (and the bottom) to give the surface  $R_{rs}$ . As shown in Baird et al. (2016), this calculation is sufficiently accurate that the primary reason for the mismatch between observed and modelled  $R_{rs}$  is errors in the coupled hydrodynamic-biogeochemical model prediction of optically-active constituents. This is, of course, the result we wanted - it means that when the assimilation system updates the optically-active biogeochemical constituents in order to minimise the mismatch between observed and modelled  $R_{rs}$ , it is changing the components of the model that have the greatest errors, and in doing so improving the solution of those parts that we most care about - the optically-active components that determine water clarity.

When testing the data assimilation system, we found that the best quantity to assimilate was the ratio of the remote-sensing reflectance at 443 and 551 nm. In fact, this ratio is the same one used in the NASA OC3M algorithm that we mentioned above is NOT a good measure of *in situ* chlorophyll in coastal waters! So how can it be that OC3M is a poor predictor of *in situ* chlorophyll in coastal waters, yet assimilating the mismatch between simulated OC3M and satellite-observed OC3M achieves the best skill for *in situ* chlorophyll when compared against independent *in situ* observations? The answer lies in that simulated OC3M is calculated using the ratio of two simulated  $R_{rs}$ , in the same manner in which observed OC3M is calculated using the ratio of two observed  $R_{rs}$ . Fig. 7 shows the *in situ* chlorophyll concentration, the simulated OC3M and the NASA observed OC3M for the Cape York region on a relatively clear day. The *in situ* chlorophyll concentration in coastal regions along this coast is  $\sim 0.5 \text{ mg m}^{-3}$  (Fig. 7 left). The simulated OC3M, calculated from simulated  $R_{rs}$ , is greater along the coastal fringe due to the absorption of blue light from CDOM, and addition bottom reflection of green light (Fig. 7 centre). The observed OC3M, also affected by CDOM absorption and the bottom, looks more like the simulated OC3M than the *in situ* chlorophyll concentration (Fig. 7 right). Further, where there are differences, the primary cause is the error in the simulated water-column optically-active constituents like chlorophyll. Thus by producing the same simulated and observed quantity, we have improved the ability of the assimilation system to update the optically-active model constituent that is in error.

OC3M uses the ratio of above-surface remote-sensing reflectance as a combination of three wavelengths,  $R'$ , which is given by:

$$R' = \log_{10} (\max [R_{rs,443}, R_{rs,488}] / R_{rs,551}) \quad (1)$$

The ratio  $R'$  is used in the OC3M algorithm to estimate surface chlorophyll,  $\text{Chl}_{OC3}$ , with coefficients from the 18 March 2010 reprocessing:

$$\text{Chl}_{OC3} = 10^{0.283 + R'(-2.753 + R'(1.457 + R'(0.659 - 1.403R')))} \quad (2)$$

obtained from [oceancolor.gsfc.nasa.gov/REPROCESSING/R2009/ocv6/](https://oceancolor.gsfc.nasa.gov/REPROCESSING/R2009/ocv6/). Using, OC3M we gain the benefit of assimilating directly the mismatch between the simulated OC3M (based on simulated remote-sensing reflectance) and the observed remote-sensing reflectance; and we use a quantity that has meaning in the water quality community (mass concentration of chlorophyll). To re-state, because we use the simulated remote-sensing reflectance to calculate OC3M, the system is not affected by the inaccuracies in the relationship between *in situ* chlorophyll and satellite-derived OC3M. And our assimilation system's prediction of chlorophyll is the simulated *in situ* chlorophyll concentration (and not OC3M).

The accuracy of the modelling systems also requires that the model and observations are closely matched in space and time. This is because remote-sensing reflectance is a function of solar angle (and therefore time of day), and because the optical properties of coastal waters can vary quickly due to a range of processes such as phytoplankton chlorophyll synthesis, movement of fronts, wind driven-upwelling, river plume structure changes etc. We used the flexible outputting time of the model, and the asynchronous assimilation routines in the EnKF-C package (Sakov, 2017), to closely align the observations and models. In doing so we were able to meet the  $\pm 30$  minutes matching requirements used for the calibration / validation of ocean colour satellite products.

The Aqua satellite overpasses the GBR between 1130 and 1530 locally. In order to match the model output to within 30 minutes of the overpass, the model remote-sensing reflectance was output at 1200, 1300, 1400 and 1500 daily. For the calculations of remote-sensing reflectance, the water column calculations of the light field (and  $R_{rs}$ ) was redone on the output time assuming the entire grid is at  $150^\circ\text{E}$ , while in fact it varies from  $142^\circ 31'\text{E}$  to  $156^\circ 51'\text{E}$ . Thus the maximum error in calculating solar angle for the purposes of outputting  $R_{rs}$ , in the Torres Strait, is about 30 minutes (this small error will be corrected in the next phase of eReefs). The light field calculation was also done at wavelengths at the centre of the MODIS ocean colour bands to avoid any small interpolations from the spectrally-resolved model that has a 20 nm resolution.

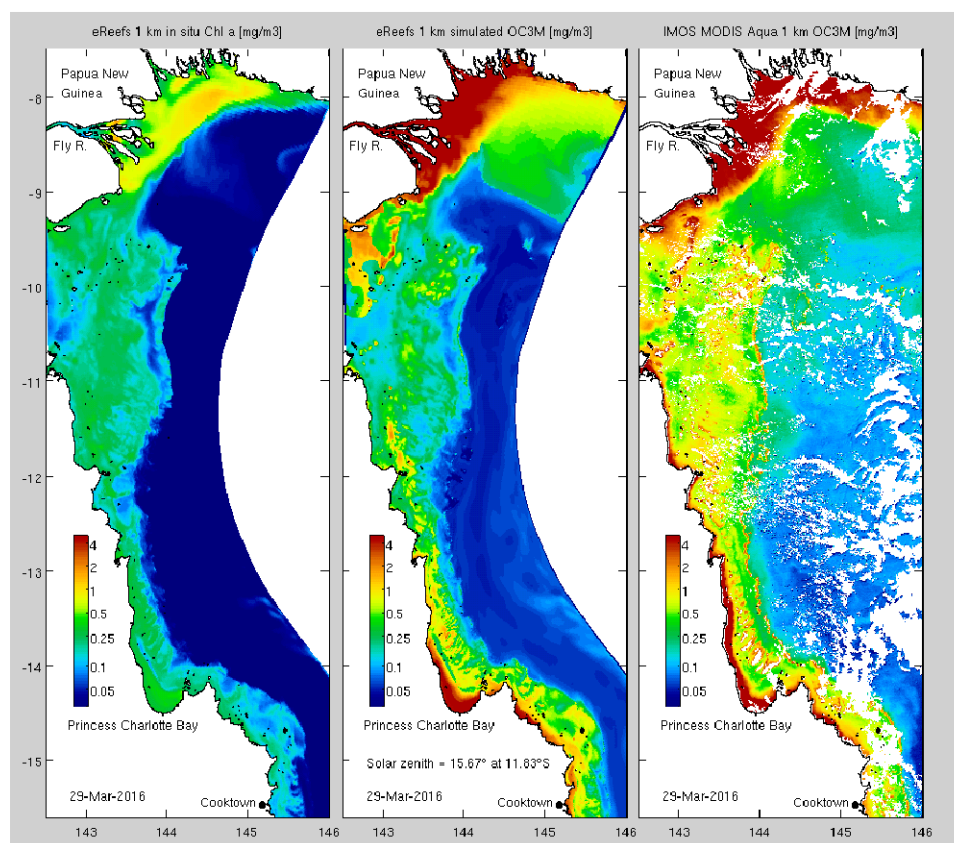


Figure 7: Example of the estimates of OC3M in the Cape York region on the 29 March 2016 using the 1 km GBR I model and the NASA Aqua MODIS sensor: *in situ* chlorophyll concentration (left), the simulated OC3M (centre) and the NASA observed OC3M (right).

The observations also need to be spatially aligned. The observations are at approximately  $\sim 1$  km resolution (up to 2 km on the edges of the swath), with location varying spatially with each different satellite swath. Meanwhile the model cells are stationary, are  $\sim 16$  km<sup>2</sup>, and are defined on the curvilinear grid. The observations are grouped into a “superobservation” for each model cell. The superobservation contains all observations that were closer to a particular cell centre than any other cell centre. The position of the superobservation is the mean of the observations it is composed of, and will be close to, but not exactly the same, as the location of the cell centre. The assimilation system then accounts for the now small misalignment in time and space when considering the mismatch between the model and observation.

### 3.5.2.2 Ensemble member design

The assimilation system used in this study is the Deterministic Ensemble Kalman Filter (DEnKF) that requires an ensemble of model runs that approximate the uncertainty in the model solution. The uncertainty in the model solution arises from uncertainty in the model initial conditions, boundary conditions, surface forcing and model parameterisations. The ensemble members differ in the values of the quadratic mortality rate coefficient of small zooplankton, in the loads of nutrients delivered in the rivers (as a multiple of the SOURCE catchments specified loads), and in the PAR light forcing (again as a multiple of the Bureau of Meteorology short wave radiation prediction). These relatively small differences, which are undertaken on the most uncertain biological parameter, and most sensitive forcing parameters, provide a spread of ensemble members that the Kalman Filter can operate on.

For a further description of the numerical schemes in the assimilation system see (Jones et al., 2016). A number of modifications have been made to improve the accuracy and efficiency of the system, including transferring the EnKF-C software.



### 3.5.3 Summary results

The non-assimilating version of the model has been compared to observations previously (ereefs.info, Baird et al. (2016) and Skerratt et al. (submitted 9 Nov. 2017)). The results produced in the reanalysis are compared directly to observations in the attached 100 page appendix showing comparisons to hundreds of time-series. Further, later components of this document compare the metric calculated using the non-assimilating model, the assimilating model, satellite observations and *in situ* observations. Here we will just show a few snapshot results to aid in the understanding of the performance of the data assimilation relative to the non-assimilating run.

#### 3.5.3.1 Assessment of chlorophyll concentration at MMP sites

In our assessment of the skill of the eReefs biogeochemical models, we have considered the most important property to be the prediction of *in situ* chlorophyll concentration at the MMP sites. For this there are two measures - the chlorophyll extractions at the sampling sites, and the calibrated chlorophyll fluorescence on the moorings. While the extractions are considered the most accurate, the fluorescence time-series is continuous. When the two are lined up in time (they are slightly separated in space), the mismatch between the observed chlorophyll extractions and the observed chlorophyll fluorescence is  $0.2 \text{ mg m}^{-3}$ . We use this  $0.2 \text{ mg m}^{-3}$  as indicative of the error of the observations.

It is important to note that the *in situ* chlorophyll concentration observations were not assimilated into the model. That is, they were observation withheld just for the model assessment. In fact, the mismatch between observed and modelled quantities used in the assimilation system is neither an *in situ* measurement, nor a chlorophyll concentration. The assimilated quantity was the ratio of remote-sensing reflectance at blue and green wavelengths. Thus, we can be confident that if the assimilation system has improved the prediction of *in situ* chlorophyll concentration then it has improved the overall biogeochemical model.

At 13 of the 14 MMP site, the assimilation of satellite-observed remote-sensing reflectance improved the prediction *in situ* chlorophyll concentration (Fig. 8, top). On average the assimilation reduced the error from  $0.34$  to  $0.29 \text{ mg m}^{-3}$ , bring it 30 % closer to the observation error (the limit of our ability to quantify an improvement in the model). The worst two site remained the most coastal sites, Geoffrey Bay and Dunk Island, for which the 4 km model poorly resolves local processes, and for which the assimilation system would provide little information to water column due to the optically-shallow and complex waters. The best site was Double Cone Island off Airlie Beach. At Double Cone Island, a time-series shows the improvement in the chlorophyll fluorescence due to the assimilation (Fig. 8, bottom). During a particularly cloud-free period in the second half of 2015, the assimilation system does a remarkable job of both removing model bias and capturing variability in the model.

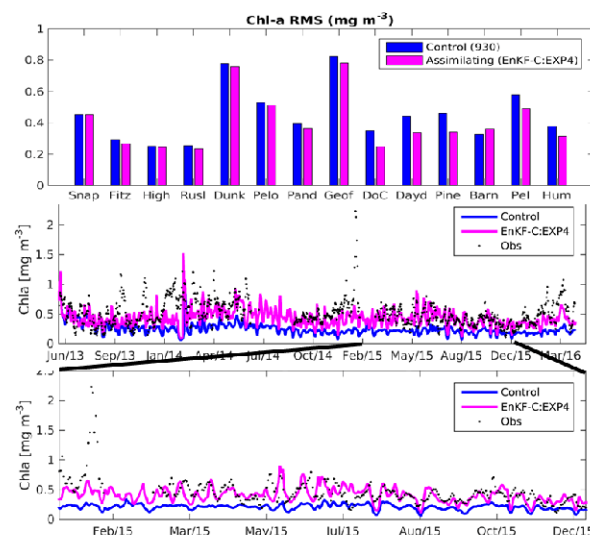


Figure 8: Comparison of the non-assimilating (blue) and assimilating (pink) runs at the MMP sites. The instantaneous state root mean square error at the 14 MMP sites (top). The approximate error in the observations is  $0.2 \text{ mg m}^{-3}$ . At Double Cone Island in the Whitsundays (off Airlie Beach), a time-series of the observations (black dots) and simulations is shown for the whole simulations (centre) and the a 1 year period (bottom).

In this context, the **eReefs** model refers to the gbr4\_bgc\_?? model (see Table?? for the catalog and model descriptions and Table7 for a description of the variables and processing).

This source of data only extends back to 2014. Whilst the eReefs GBR4\_BGC\_? model technically does contain 2013 calendar year data, the current project partitions time into water years in which the full 2013 water year starts in October 2012. Therefore as the 2013 is not a complete 12 months of data, it is excluded from analyses. Unfortunately, this means that any signals associated with the 2010-2011 floods are unavailable.

Table 7: Measures collected from eReefs assimilated model. Data used are daily means per pixel. Variable and Description pertain to the eReefs source. Conversion indicates the conversion applied on data to conform to threshold Units. Abbreviation provides a consistent key across data.

Measure	Variable	Description	Abbreviation	Conversion	Units
Chlorophyll-a	Chl_a_um	Sum of Chlorophyll concentration of four microalgae types ( $mg/m^3$ )	chl	Chl_a_um x1	$\mu gL^{-1}$
Non-Algal Particles	EFI	??	nap	EFI x1000	$mgL^{-1}$
Secchi Depth	Kd_490	??	sd	1/Kd_490	m
NOx	NO3	Concentration of Nitrate. As Nitrite is not represented in the model, NO3 = $[NO_3^-] + [NO_2^-]$ ( $mg/m^3$ )	NOx	NO3 x1	$\mu gL^{-1}$

### 3.6 eReefs926

In this context, the **eReefs926** model refers to the gbr4\_bgc\_926 model (see Table??). This model provides alternative formulation and importantly does extend back to the full 2013 water year thereby providing some coverage closer to the 2010-2011 flood period.

Variables used as per Table 7

### 3.7 Thresholds

An environmental health metric represents the state or condition relative to some reference, threshold or expectation. Most of the current water quality indices compare values to a set of specifically selected *guidelines*. These guidelines are either formulated specifically from long-term historical data appropriate to the spatial and temporal domain of interest or else are based on ANZEC guidelines (Australian and New Zealand Environment and Conservation Council, 2000).

Typically there are strict guidelines on how these guidelines should be applied. In particular, the guidelines associated with various measures used in various report cards throughout the Great Barrier Reef should be applied to annually aggregated data - not individual observations. Since this project intends to generate indices on the scale of individual observations, we have decided to refer to the guidelines as *thresholds* so as to avoid contradicting the terms of use of guidelines..

The thresholds used for each Measure within each Region and Water body are indicated in Table A1 (page 177). Note, that whilst the application of seasonal thresholds could potentially remove some uncertainty, in the absence of clear consensus on how to define wet and dry seasons and what the associated set of thresholds would be, seasonal thresholds are not used in this project.